

Crystal structure and magnetic properties of a cyano-bridged bimetallic assembly $[\text{CuL}^4]_3[\text{Fe}(\text{CN})_6]_2 \cdot 2\text{H}_2\text{O}$ ($\text{L}^4 = 3,10$ -dibutyl-1,3,5,8,10,12-hexaazacyclotetradecane)

Xiao-Ping Shen^{a,b,*}, Yi Xu^a, Hu Zhou^c, He-Qing Shu^a, Ai-Hua Yuan^c

^a School of Chemistry and Chemical Engineering, Jiangsu University, Zhenjiang 212013, PR China

^b State Key Laboratory of Coordination Chemistry, Nanjing University, Nanjing 210093, PR China

^c School of Material Science and Engineering, Jiangsu University of Science and Technology, Zhenjiang 212003, PR China

ARTICLE INFO

Article history:

Received 12 March 2008

Received in revised form 22 April 2008

Accepted 28 April 2008

Available online 10 May 2008

Keywords:

Hexacyanoferrate(III)

Copper complex

Cyano-bridged complex

Crystal structure

Magnetic properties

ABSTRACT

A novel cyano-bridged bimetallic assembly $[\text{CuL}^4]_3[\text{Fe}(\text{CN})_6]_2 \cdot 2\text{H}_2\text{O}$ (**1**) ($\text{L}^4 = 3,10$ -dibutyl-1,3,5,8,10,12-hexaazacyclotetradecane), which was prepared by self-assembly of $[\text{Fe}(\text{CN})_6]^{3-}$ and $[\text{CuL}^4]^{2+}$, has been characterized by elemental analyses, ICP, IR, single crystal X-ray structure analysis and magnetic measurements. The structure of complex **1** consists of two distinct neutral moieties: one is a two-dimensional (2-D) polymeric layer and the other is a pentanuclear Cu_3Fe_2 short chain, which are supramolecular isomers and result from two different coordination modes of $[\text{Fe}(\text{CN})_6]^{3-}$ via the $\text{Fe}-\text{C}\equiv\text{N}-\text{Cu}$ linkages. Magnetic studies reveal the presence of a weak antiferromagnetic interactions between the adjacent copper(II) and iron(III) ions through cyano bridges.

© 2008 Elsevier B.V. All rights reserved.

1. Introduction

There has been continuous interest in design and construction of polymetallic extended compounds [1–2] because of their potential applications for technologically useful magnetic, electronic, optical, electrochemical and catalytic materials. Especially, much effort has been made for the design of highly ordered structures with paramagnetic metal centers in order to provide molecular-based magnets exhibiting spontaneous magnetization. It is known that cyanide-bridged bimetallic assemblies, derived from $[\text{M}(\text{CN})_6]^{n-}$ ($\text{M} = \text{Fe}, \text{Cr}, \text{Mn}, \text{Co}$) building blocks and coordinatively unsaturated transition metal complexes, exhibit ferro-, ferri-, and meta-magnetic behavior and form a family of magnetic materials [3–4]. For instance, Okawa and coworkers reported two three-dimensional (3-D) Mn_3Cr_2 ferrimagnets, $[\text{Mn}(\text{en})_3][\text{Cr}(\text{CN})_6]_2 \cdot 4\text{H}_2\text{O}$ [5] and $[\text{Mn}(\text{glya})_3][\text{Cr}(\text{CN})_6]_2 \cdot 2.5\text{H}_2\text{O}$ [6] (glya = glycineamide), which show magnetic ordering at $T_C = 69$ and 71 K, respectively. Since copper(II) normally possesses four-, five-, or six-coordination, it is anticipated that the coupling of the copper complexes with hexacyanometalates can give rise to a large variety of assembled complexes with rich structural architectures and

tunable physical properties. In 2001, Gao et al. reported a unique 3-D coordination polymer $[\text{Cu}(\text{EtOH})][\text{Cu}(\text{en})_2][\text{Cr}(\text{CN})_6]_2$ with ferromagnetic ordering below 57 K [7]. Recently, we reported a ferromagnetic cyano-bridged 3-D assembly $[\text{CuL}^3]_2[\text{Cr}(\text{CN})_6]\text{ClO}_4 \cdot 0.5\text{H}_2\text{O}$ using a Cu(II) macrocyclic complex $[\text{CuL}^3]^{2+}$ as a building block ($\text{L}^3 = 3,10$ -dipropyl-1,3,5,8,10,12-hexaazacyclotetradecane) [8]. As an extend of our previous work, we have synthesized a new cyano-bridged Cu(II)–Fe(III) assembly of $[\text{CuL}^4]_3[\text{Fe}(\text{CN})_6]_2 \cdot 2\text{H}_2\text{O}$ (**1**) using another macrocyclic building block $[\text{CuL}^4]^{2+}$ ($\text{L}^4 = 3,10$ -dibutyl-1,3,5,8,10,12-hexaazacyclotetradecane). In this paper, its synthesis, crystal structure and magnetic properties are reported.

2. Experimental

2.1. Physical measurements

Elemental analyses for C, H and N were performed at a Perkin-Elmer 240C analyzer. Cu and Fe analyses were made on a Jarrell-Ash 1100 + 2000 inductively coupled plasma spectrometer. IR spectra were recorded on a Nicolet FT-170SX spectrometer with KBr pellets in the 4000–400 cm^{-1} region. The magnetic measurements were performed using a Quantum Design MPMS-XL SQUID magnetometer. Diamagnetic corrections were made using Pascal's constants. Effective magnetic moments were calculated using the equation $\mu_{\text{eff}} = 2.828(\chi_M \times T)^{1/2}$, where χ_M is the magnetic susceptibility per formula unit.

* Corresponding author. Address: School of Chemistry and Chemical Engineering, Jiangsu University, Zhenjiang 212013, PR China. Tel.: +86 511 83593133; fax: +86 511 88791800.

E-mail address: xiaopingshen@163.com (X.-P. Shen).

2.2. Preparations

All chemicals and solvents were reagent grade and were used without further purification. The Cu(II) macrocyclic complex $[\text{CuL}^4](\text{ClO}_4)_2$ was synthesized according to the method reported previously [9].

2.2.1. Caution

Perchlorate salts of metal complexes with organic ligands are potentially explosive and should be handled in small quantities with great care.

2.2.2. $[\text{CuL}^4]_3[\text{Fe}(\text{CN})_6]_2 \cdot 2\text{H}_2\text{O}$ (**1**)

Complex **1** was obtained as purplish-red single crystals by slow diffusion of a DMF solution (15 cm^3) of $[\text{CuL}^4](\text{ClO}_4)_2$ (0.15 mmol) and an aqueous solution (15 cm^3) of $\text{K}_3[\text{Fe}(\text{CN})_6]$ (0.15 mmol) through a U-shaped tube containing silica gel at room temperature. The resulting crystals were collected, washed with H_2O and EtOH, respectively, and dried in air. It is insoluble in most inorganic and organic solvents. Anal. found: C, 45.15; H, 7.33; N, 26.48; Fe, 6.92; Cu, 12.07%. Calc. for $\text{C}_{60}\text{H}_{118}\text{Cu}_3\text{Fe}_2\text{N}_{30}\text{O}_2$: C, 45.20; H, 7.46; N,

26.36; Fe, 7.00; Cu, 11.96%. IR: $\nu_{\text{max}}/\text{cm}^{-1}$ 3418(s), 3240(s), 2957(s), 2933(s), 2872(s), 2116(s), 2103(s), 1628(m), 1467(m), 1426(m), 1281(m), 1086(m), 1062(s), 1018(vs), 940(m), 886(m), 626(m), 440(w).

2.3. Crystallography

Diffraction data were collected at 293 K on a Bruker SMART APEX CCD area detector diffractometer using graphite-monochromated Mo- $K\alpha$ radiation ($\lambda = 0.71073 \text{ \AA}$) with the φ and ω scan mode. Empirical absorption correction was made with SADABS. The structure was solved by direct methods and refined by full matrix least-squares techniques based on F^2 . All non-hydrogen atoms were refined with anisotropic thermal parameters. The idealized positions of the hydrogen atoms were located by using a riding model. All computations were carried out using the SHELXTL-PC program package.

Crystal data for **1**: $\text{C}_{60}\text{H}_{118}\text{Cu}_3\text{Fe}_2\text{N}_{30}\text{O}_2$, $M = 1594.16$, monoclinic, space group $P2(1)/c$ (No. 14), $a = 17.3263(13)$, $b = 29.227(2)$, $c = 17.3263(13) \text{ \AA}$, $\beta = 115.021(5)^\circ$, $U = 7950.6(11) \text{ \AA}^3$, $Z = 4$, $D_c = 1.332 \text{ g/cm}^3$, $F(000) = 3372$, $\mu = 1.204 \text{ mm}^{-1}$ and $S = 1.07$.

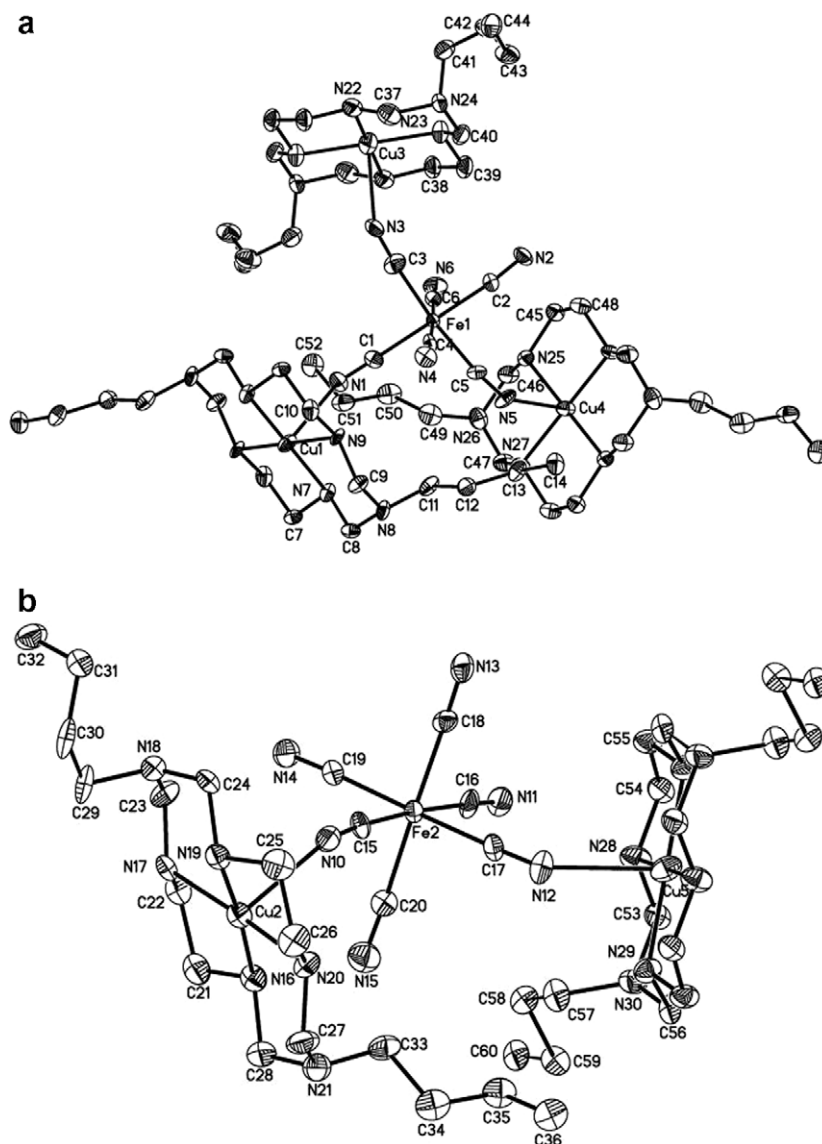


Fig. 1. ORTEP views of complex **1** for (a) 2D layer and (b) pentanuclear chain moieties with the atom numbering scheme. Water molecule is omitted for clarity.

About 42,468 reflections measured, 15550 unique ($R_{\text{int}} = 0.040$). The final $R_1 = 0.0542$ and $wR_2 = 0.1336$ for 11927 observed reflections [$I > 2\sigma(I)$] and 885 parameters.

3. Results and discussion

3.1. Crystal structure

The structure of complex **1** is shown in Figs. 1–3. The selected bond distances and angles are listed in Table 1. The molecular structure of complex **1** consists of two distinct neutral moieties. One is a 2-D polymeric layer, the other is a discrete Cu_3Fe_2 pentanuclear chain-like unit. As shown in Fig. 1a, each $[\text{Fe}(\text{CN})_6]^{3-}$ anion within the 2-D layer coordinates with three $[\text{CuL}^4]^{2+}$ cations (Cu1, Cu3 and Cu4) via three *mer*- $\text{C}\equiv\text{N}$ groups, whereas each $[\text{CuL}^4]^{2+}$ cation is linked to two symmetry-related $[\text{Fe}(\text{CN})_6]^{3-}$ ions in *trans* positions, which leads to a 2-D neutral network structure consisting of ring-like dodecanuclear $[-\text{Fe}-\text{CN}-\text{Cu}-]_6$ units in *ac* plane

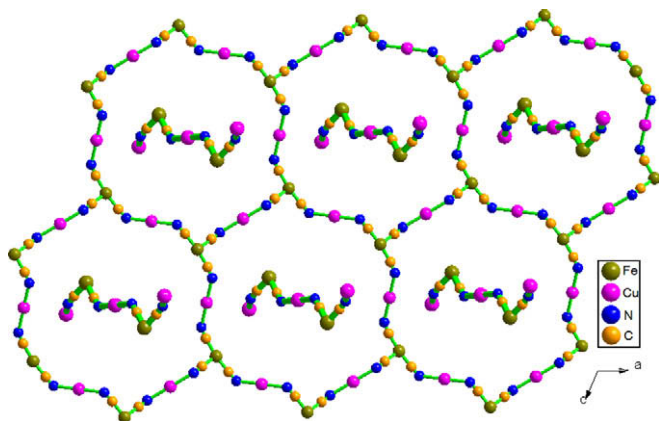


Fig. 2. Projection of complex **1** along the *b*-axis, showing the layer structure with discrete pentanuclear units. Only metal ions and bridged-CN are shown for clarity.

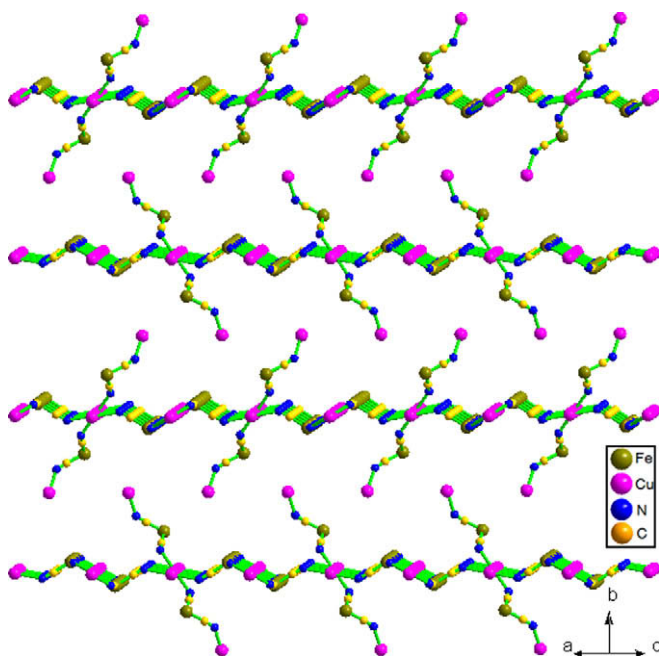


Fig. 3. Packing diagram of complex **1** viewed from the *a*-axis, only metal ions and bridged-CN are shown for clarity.

Table 1
Selected bond distances (Å) and bond angles (°) for complex **1**

Bond distances			
Cu1–N1	2.594(4)	Cu4–N27	2.043(3)
Cu1–N7	2.007(3)	Cu4–N5C	2.588(3)
Cu1–N9	2.012(3)	Cu4–N25C	1.998(3)
Cu1–N1B	2.594(4)	Cu4–N27C	2.043(3)
Cu1–N7B	2.007(3)	Cu5–N29	2.003(3)
Cu1–N9B	2.012(3)	Cu5–N12	2.537(4)
Cu3–N3	2.619(4)	Cu5–N28	2.028(3)
Cu3–N22	1.999(4)	Cu5–N12D	2.537(4)
Cu3–N23	2.001(3)	Cu5–N28D	2.028(3)
Cu3–N3A	2.619(4)	Cu5–N29D	2.003(3)
Cu3–N22A	1.999(4)	Cu2–N17	2.021(3)
Cu3–N23A	2.001(3)	Cu2–N10	2.372(3)
Cu4–N5	2.588(3)	Cu2–N16	2.019(4)
Cu4–N25	1.998(3)	Cu2–N19	2.023(3)
		Cu2–N20	2.018(3)
Bond angles			
Fe1–C1–N1	175.0(3)	Fe1–C3–N3	175.4(4)
Fe1–C2–N2	172.5(3)	Fe1–C4–N4	176.8(3)
Fe1–C5–N5	172.2(3)	Fe1–C6–N6	177.3(3)
C1–Fe1–C4	84.64(15)	C1–Fe1–C5	94.68(14)
C1–Fe1–C3	90.39(17)	C1–Fe1–C6	92.86(15)
C2–Fe1–C3	88.54(17)	C3–Fe1–C6	85.49(17)
C2–Fe1–C4	90.08(15)	C1–Fe1–C2	174.53(15)
C2–Fe1–C6	92.40(15)	C4–Fe1–C5	93.44(14)
C3–Fe1–C4	94.24(17)	C4–Fe1–C6	177.49(15)
C3–Fe1–C5	171.16(18)	C2–Fe1–C5	87.07(14)
Fe2–C15–N10	174.2(3)	Fe2–C16–N11	177.9(3)
Fe2–C17–N12	177.5(3)	Fe2–C18–N13	176.3(3)
Fe2–C19–N14	176.8(3)	Fe2–C20–N15	176.3(4)
C15–Fe2–C18	92.96(15)	C15–Fe2–C16	176.23(15)
C15–Fe2–C20	85.96(15)	C16–Fe2–C17	89.70(14)
C18–Fe2–C20	177.77(14)	C19–Fe2–C20	89.34(15)
C15–Fe2–C19	90.65(14)	C16–Fe2–C18	90.53(15)
C16–Fe2–C19	90.61(14)	C16–Fe2–C20	90.50(15)
C17–Fe2–C18	86.12(14)	C17–Fe2–C19	178.72(16)
Cu1–N1–C1	141.6(3)	Cu2–N10–C15	141.6(3)
Cu3–N3–C3	134.0(3)	Cu4–N5–C5	140.5(3)
Cu5–N12–C17	130.9(3)	N5–Cu4–N5C	180.00
N1–Cu1–N1B	180.00	N12–Cu5–N12D	180.00
N3–Cu3–N3A	180.00		

Symmetry transformations used to generate equivalent atoms: $A = -x, -y, -z$; $B = 1-x, -y, -z$; $C = 1-x, -y, 1-z$; $D = -x, 2-y, 1-z$.

(Fig. 2). The three independent Cu^{II} ions (Cu1, Cu3 and Cu4) all assume elongated octahedral coordination configurations, in which the equatorial sites are occupied by four nitrogen atoms of the macrocyclic ligand L^4 with the $\text{Cu}-\text{N}_{\text{eq}}$ bond distances in the range of 1.998(3)–2.043(3) Å, while the axial positions are occupied by two nitrogen atoms from CN^- groups with the $\text{Cu}-\text{N}_{\text{ax}}$ distances of 2.588(3)–2.619(4) Å. The fact that the $\text{Cu}-\text{N}_{\text{ax}}$ distances are much longer than the $\text{Cu}-\text{N}_{\text{eq}}$ bond distances can be attributed to the Jahn–Teller effects of Cu^{II} ion and has been observed in many other cyanometalate analogs [8,10–12], such as $[\text{Cu}(\text{en})_2]_3$ $[\text{W}(\text{CN})_8]_2 \cdot \text{H}_2\text{O}$ [10] with $\text{Cu}-\text{N}_{\text{ax}}$ distances of 2.329(6)–2.967(7) Å and $[\text{CuL}^3]_2[\text{Cr}(\text{CN})_6]\text{ClO}_4 \cdot 0.5 \text{H}_2\text{O}$ [8] with $\text{Cu}-\text{N}_{\text{ax}}$ distances of 2.539 and 2.577 Å. In addition, the $\text{Cu}-\text{N}-\text{C}$ bond angles are far from linearity with the angles of $\text{Cu1}-\text{N1}-\text{C1} = 141.56$, $\text{Cu3}-\text{N3}-\text{C3} = 134.04$ and $\text{Cu4}-\text{N5}-\text{C5} = 136.05^\circ$.

As shown in Fig. 1b, in the discrete pentanuclear structural unit, each $[\text{Fe}(\text{CN})_6]^{3-}$ anion is linked to two $[\text{CuL}^4]^{2+}$ cations by using two *cis*- $\text{C}\equiv\text{N}$ groups, whereas $[\text{CuL}^4]^{2+}$ cations can be divided into two different types according to their bonding mode with $[\text{Fe}(\text{CN})_6]^{3-}$. The Cu5 ion coordinates with two symmetry-related $[\text{Fe}(\text{CN})_6]^{3-}$ ions in *trans* positions, and assumes a distorted octahedral geometry with the equatorial sites occupied by four nitrogen atoms of the macrocyclic ligand L^4 and the axial positions occupied by two nitrogen atoms from CN^- groups. The Cu2 ion is pentacoordinate and presents a square-based pyramidal configuration in which the four N atoms from the macrocyclic ligand L^4 constitute

the basal plane while the apical position is occupied by the N atom from cyanide group of $[\text{Fe}(\text{CN})_6]^{3-}$. Since the Cu coordinates with only one $[\text{Fe}(\text{CN})_6]^{3-}$ ion, the Cu—C≡N—Fe linkage is terminated in Cu2 and forms a Cu_3Fe_2 pentanuclear short chain structure (Fig. 2). As the case mentioned above, due to the Jahn–Teller effects, the Cu5— N_{ax} distances of 2.537 Å are much longer than the Cu5— N_{eq} bond distances of 2.003 and 2.028 Å, leading to an elongated octahedron. The distances of basal Cu2—N bonds are in the range 2.018–2.023 Å, which is shorter than the distance 2.372 Å of the apical Cu2—N bond. The Cu—N≡C bond angles are far from linearity with the angles of Cu2—N10—C15 = 141.6(3) and Cu5≡N12≡C17 = 130.9(3)°.

As usual, the $[\text{Fe}(\text{CN})_6]^{3-}$ fragments, both in the polymeric layer and in the discrete pentanuclear chain, exhibit a distorted octahedral structure. The cis-C—Fe—C bond angles are in the range 84.6–94.7° for Fe1 and 86.0–93.0° for Fe2. The Fe—C≡N angles are slightly bent (172.3–177.3° for Fe1 and 174.2–177.9° for Fe2). The Fe—C distances for the Fe1 (1.895–1.946 Å) are slightly shorter than those for the Fe2 (1.910–1.973 Å), while the C≡N distances for the Fe1 (1.136–1.176 Å) are slightly longer than those for the Fe2 (1.106–1.166 Å). The Fe...Cu distances through the cyanide bridges are Fe1...Cu1 = 5.321, Fe1...Cu3 = 5.194, Fe1...Cu4 = 5.244, Fe2...Cu2 = 5.056 and Fe2...Cu5 = 5.068 Å, respectively. The polymeric layers (Fig. 3) show a —ABAB— packing mode and the pentanuclear short chains can run through the layers via the cavities of the dodecanuclear $[-\text{Fe}-\text{CN}-\text{Cu}-]_6$ rings. There are a number of hydrogen bonds among the lattice water molecule, the terminal CN^- nitrogen, and the nitrogen of the macrocyclic ligand L^4 (Table 2), which connect the 2-D layer, pentanuclear chain and lattice water together to form a pseudo-three-dimensional crystal structure. In addition, the bonding parameters of the macrocyclic ligand L^4 are close to those found in related complexes reported previously [8,13–14].

It should be pointed out that in the $[\text{Fe}(\text{CN})_6]^{3-}/[\text{ML}]^{2+}$ ($\text{M} = \text{Ni}, \text{Cu}$; $\text{L} = 3,10$ -disubstituted-1,3,5,8,10,12-hexaazacyclotetradecane) adducts, the $[\text{Fe}(\text{CN})_6]^{3-}$ can show different coordination modes depending on the substituted pendant of ligand L. For example, in the complex of $[\text{NiL}^1]_3[\text{Fe}(\text{CN})_6]_2 \cdot 9\text{H}_2\text{O}$ [15] ($\text{L}^1 = 3,10$ -dimethyl-1,3,5,8,10,12-hexaazacyclotetradecane), each $[\text{Fe}(\text{CN})_6]^{3-}$ anion connects three nickel(II) ions using three *fac*-C≡N groups, which results in a 2-D stair-shaped honeycomb-like structure, whereas using ligand L^2 ($\text{L}^2 = 3,10$ -diethyl-1,3,5,8,10,12-hexaazacyclotetradecane) instead of L^1 , the complex $[\text{NiL}^2]_3[\text{Fe}(\text{CN})_6]_2 \cdot 12\text{H}_2\text{O}$ [16] is obtained with completely different flat brick wall-like structure, in which each $[\text{Fe}(\text{CN})_6]^{3-}$ anion coordinates with three nickel(II) ions using three *mer*-C≡N groups. In our present case, when using ligand L^3 ($\text{L}^3 = 3,10$ -dipropyl-1,3,5,8,10,12-hexaazacyclotetradecane) instead of L^4 , the complex of $[\text{CuL}^3]_2[\text{Fe}(\text{CN})_6]_2 \cdot \text{ClO}_4 \cdot 4\text{H}_2\text{O}$ [17] with a 3-D structure is obtained, in which each $[\text{Fe}(\text{CN})_6]^{3-}$ ion connects four copper(II) ions using four co-planar CN^- groups. Therefore, by rationally modifying

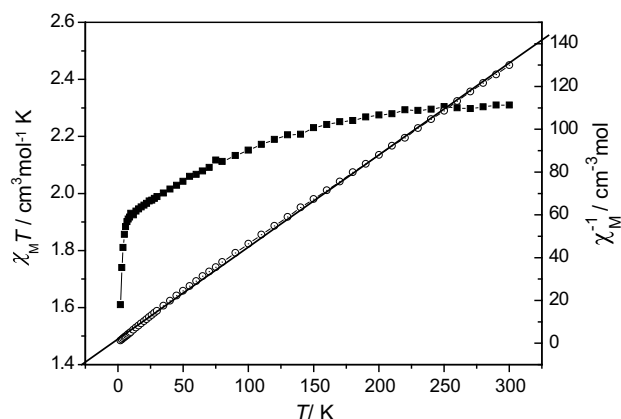


Fig. 4. Temperature dependence of $\chi_M T$ (■) and $1/\chi_M$ (○) for complex **1** measured at 2 kOe. The solid line represents the fit obtained by the Curie–Weiss law (see text).

organic ligands, it is possible to synthesize complexes with various molecular structures, which is advantaged to achieve expected physical and chemical properties.

3.2. Magnetic properties

The magnetic susceptibilities of complex **1** were measured with an applied field $H = 2$ kOe in the temperature range 2–300 K. The plots of $\chi_M T$ vs. T and $1/\chi_M$ vs. T are given in Fig. 4. At room temperature, the $\chi_M T$ per Cu_3Fe_2 unit is $2.3 \text{ cm}^3 \text{ K mol}^{-1}$ ($4.3 \mu_B$), which is bigger than the spin-only value of $1.88 \text{ cm}^3 \text{ K mol}^{-1}$ ($3.87 \mu_B$) expected for an uncoupled spin system (three $S_{\text{Cu}} = 1/2$, two $S_{\text{Fe}} = 1/2$) with $g = 2.0$. This is likely due to the orbital contribution to the magnetic moment of the low-spin Fe^{III} . On lowering the temperature, the $\chi_M T$ value monotonically decreases, first gradually till ca. 10 K and then sharply down to a value of $1.61 \text{ cm}^3 \text{ K mol}^{-1}$ ($3.59 \mu_B$) at 2 K. The slow decrease of $\chi_M T$ above 10 K is characteristic of a low spin octahedral Fe^{III} system with spin-orbital coupling of the ${}^2T_{2g}$ ground term [12], while the fast decrease of $\chi_M T$ below 10 K suggests an antiferromagnetic coupling between copper(II) and iron(III) ions through cyano bridges. The plot of $1/\chi_M$ vs. T obeys the Curie–Weiss law with a negative Weiss constant = -4.5 K, confirming further the presence of a weak antiferromagnetic interaction in complex **1**. According to the orthogonality theory of magnetic orbitals [18], the magnetic interaction between Cu^{II} ($d_{x^2-y^2}$) and Fe^{III} (t_{2g}^5) should be ferromagnetic. The antiferromagnetic interaction in complex **1** probably results from the nonlinear Cu—N≡C angles, which can break down the strict orthogonality of the $d_{x^2-y^2}$ and t_{2g} magnetic orbitals. In addition, both the nonlinear Cu—N≡C angles and the long Cu— $\text{N}_{\text{cyanide}}$ bond distances can markedly weaken the magnetic coupling through the Fe—C≡N—Cu linkages and leads to a weak magnetic interaction in complex **1**.

4. Conclusion

A novel cyano-bridged bimetallic assembly, $[\text{CuL}^4]_3[\text{Fe}(\text{CN})_6]_2 \cdot 2\text{H}_2\text{O}$, has been synthesized and characterized structurally and magnetically. It has a unique polymeric structure consisting of a 2D infinite layer and a pentanuclear finite chain, which result from two different coordination modes of $[\text{Fe}(\text{CN})_6]^{3-}$, respectively. The presence of 2D layers and pentanuclear moieties is the first observation in cyanide-bridged bimetallic complexes. The present research clearly shows that the rational modification of organic ligands should bring about the modification of molecular structures and further illustrates the structural diversity of bimetallic assemblies constructed from hexacyanometalates and copper(II) complexes. Magnetic studies on this complex reveal

Table 2
Hydrogen-bond geometry (Å, °)

D—H...A	D—H	H...A	D...A	D—H...A
O1—H1D...N11	0.85	1.71	2.555(4)	178
O2—H2B...N2	0.85	2.2	2.859(5)	134
N9—H9...N4	0.91	2.49	3.282(5)	146
N16—H16A...N15	0.91	2.38	3.211(6)	152
N17—H17A...N4	0.91	2.34	3.091(4)	140
N19—H19A...N14	0.91	2.28	3.138(4)	158
N20—H20A...O2	0.91	2.26	3.135(4)	160
N22—H22C...N6	0.91	2.61	3.304(5)	134
N25—H25C...N6	0.91	2.52	3.283(4)	142
N27—H27C...N13	0.91	2.51	3.278(5)	142
N28—H28C...N11	0.91	2.43	3.156(5)	137

the presence of a weak antiferromagnetic interactions between the adjacent copper(II) and iron(III) ions through cyano bridges.

5. Supplementary materials

CCDC 661777 contains the supplementary crystallographic data for this paper. These data can be obtained free of charge via www.ccdc.cam.ac.uk/conts/retrieving.html (or from the Cambridge Crystallographic Data Centre, 12, Union Road, Cambridge CB2 1EZ, UK; fax: +44 1223 336033).

Acknowledgments

This work was supported by the Natural Science Foundation of Jiangsu Province (No. BK2005056) and the Foundation of State Key Laboratory of Coordination Chemistry.

References

- [1] C.T. Chen, K.S. Suslick, *Coord. Chem. Rev.* 128 (1993) 293.
- [2] O.M. Yaghi, M. O'Keeffe, M. Kanatzidis, *J. Solid State Chem.* 152 (2000) 1.
- [3] M. Ohba, H. Okawa, *Coord. Chem. Rev.* 198 (2000) 313.
- [4] J. Cernak, M. Orendac, I. Potocnak, J. Chomic, A. Orendacova, J. Skorsepa, A. Feher, *Coord. Chem. Rev.* 224 (2002) 51.
- [5] M. Ohba, N. Usuki, N. Fukita, H. Okawa, *Angew. Chem. Int. Ed.* 38 (1999) 1795.
- [6] N. Usuki, M. Yamada, M. Ohba, H. Okawa, *J. Solid State Chem.* 159 (2001) 328.
- [7] H.Z. Kou, S. Gao, J. Zhang, G.H. Wen, G. Su, R.K. Zheng, X.X. Zhang, *J. Am. Chem. Soc.* 123 (2001) 11809.
- [8] X.P. Shen, S. Gao, G. Yin, K.B. Yu, Z. Xu, *New J. Chem.* 28 (2004) 996.
- [9] M.P. Suh, S.G. Kang, *Inorg. Chem.* 27 (1988) 2544.
- [10] D.F. Li, S. Gao, L.M. Zheng, W.Y. Sun, T. Okamura, N. Ueyama, W.X. Tang, *New J. Chem.* 26 (2002) 485.
- [11] H.Z. Kou, H.M. Wang, D.Z. Liao, P. Cheng, Z.H. Jiang, S.P. Yan, X.Y. Huang, G.L. Wang, *Aust. J. Chem.* 51 (1998) 661.
- [12] E. Colacio, J.M. Dominguez-Vera, M. Ghazi, R. Kivekas, J.M. Moreno, A. Pajunen, *J. Chem. Soc. Dalton Trans.* (2000) 505.
- [13] H.Z. Kou, S. Gao, O. Bai, Z.M. Wang, *Inorg. Chem.* 40 (2001) 6287.
- [14] H.Z. Kou, W.M. Bu, S. Gao, D.Z. Liao, Z.H. Jiang, S.P. Yan, Y.G. Fan, G.L. Wang, *J. Chem. Soc. Dalton Trans.* (2000) 2996.
- [15] H.Z. Kou, S. Gao, W.M. Bu, D.Z. Liao, B.Q. Ma, Z.H. Jiang, S.P. Yan, Y.G. Fan, G.L. Wang, *J. Chem. Soc. Dalton Trans.* (1999) 2477.
- [16] H.Z. Kou, S. Gao, B.Q. Ma, D.Z. Liao, *Chem. Commun.* (2000) 1309.
- [17] A.H. Yuan, X.P. Shen, H. Zhou, *Transition Met. Chem.* 33 (2008) 133.
- [18] M. Verdaguier, A. Bleuzen, V. Marvaud, J. Vaissermann, M. Seuleiman, C. Desplanches, A. Scuille, C. Train, R. Garde, G. Gelly, C. Lomenech, I. Rosenman, P. Veillet, C. Cartier, F. Villain, *Coord. Chem. Rev.* 190–192 (1999) 1023.